Dependence of T_c on normal and magnetic impurities in the hole mechanism of superconductivity

F. Marsiglio
Theoretical Physics Branch, Chalk River Laboratories, AECL Research, Chalk River, Ontario, Canada K0J 1J0
(Received 13 May 1991)

The influence of impurities on the superconducting transition temperature including effects of the finite bandwidth is investigated. The attractive Hubbard model is treated first, where it is found that normal impurities are pair breaking for narrow bands. Nonetheless, magnetic impurities are almost always significantly more pair breaking. Then we investigate a recently proposed model for superconductivity in the high-T_c oxides, the hole mechanism. It is found that for the relevant parameter regime of the high-T_c oxides, normal and magnetic impurities are equally pair breaking. This behavior is in qualitative agreement with transition-metal-doping experiments.

I. INTRODUCTION

Since the discovery of the high-T_c oxides several kinds of substitution experiments have been attempted. These include rare-earth substitutions (e.g., Eu for Y in $YBa_2Cu_3O_{7-u}$), doping substitutions (e.g., Sr for La in $La_{2-y}Sr_yCuO_4$), and transition-metal substitutions (e.g., Ni or Zn for Cu in either of the above compounds). The first kind of substitution has almost no effect on T_c, presumably because the rare-earth site is well removed from the hole-conduction paths. The case of Pr for Y remains an intriguing exception. Superconductivity is actually achieved by the second category of substitution. In the $La_{2-y}Sr_yCuO_4$ compounds, T_c vs y has the shape of an inverted parabola,[1-3] with maximum T_c near $y \sim 0.15$.

The third kind of substitution presumably creates scattering centers for the relevant conduction holes without increasing or depleting the hole concentration. It is found experimentally that T_c is significantly reduced by *both*[4,5] normal- (nonmagnetic) *and* by magnetic-ion substitutions. Moreover the T_c reduction is approximately the same in both cases. The conventional theory of superconductivity maintains that normal impurities have little or no effect on T_c,[6] whereas magnetic impurities quickly suppress T_c.[7] It is therefore important to try to understand this behavior in the context of different theoretical proposals for high T_c.

At the same time it is important to realize that the aforementioned "conventional" behavior of T_c with respect to impurity doping is a *weak-coupling* result. As we shall see, removing this assumption alters the picture significantly. Normal impurities become pair breaking, but never to the extent that magnetic impurities are. These results will be outlined in Sec. III, after the necessary theoretical formalism has been introduced in Sec. II. In Sec. IV the dependence of T_c on impurities is discussed in the context of the hole mechanism[8] of superconductivity. Many of the implications of this theory have already been presented in Ref. 9. T_c is driven by a term in the Hamiltonian that modulates the hopping of electrons due to the presence of other electrons in the vicinity. In a single-band picture, T_c is nonzero only when the chemical potential lies in a regime where the hole picture is more appropriate—hence the name "hole mechanism." In the remainder of this paper we therefore adopt the hole representation. Similar ideas have been discussed recently by other authors as well.[10-12] One important result is that the effective potential between two holes is momentum dependent, through the hole kinetic energy. This in turn leads to a pairing function, Δ_k, which is also dependent on the hole kinetic energy[9]:

$$\Delta_k = \Delta_0 - \frac{\varepsilon_k}{D/2}\Delta_1 \ . \tag{1}$$

Since the pairing potential between two quasiparticles is significant throughout the Brillouin zone, and not just at the Fermi surface, Anderson's argument[6] no longer holds and one expects normal impurities to affect T_c. Indeed, a similar momentum dependence in the pairing function is obtained in the mean-field treatment of the resonating-valence-bond theory.[13-14] There it has been noted[15] that normal impurities have a pair-breaking effect, analogous to that of magnetic impurities. We find this to be the case here, and indeed, over a wide parameter range, we find that normal and magnetic impurities are equally pair breaking. Finally, in Sec. V, we conclude with a summary.

II. BCS EQUATIONS

Using the reduced hole mechanism Hamiltonian previously defined in Ref. 9, and following the treatment of Allen and Mitrović,[18] we obtain the following equations:

$$Z(k,i\omega_m) = 1 + \frac{1}{N}\sum_{k'}\frac{t_+(k,k')}{N(\mu)}\frac{Z(k',i\omega_m)}{\omega_m^2 Z^2(k',i\omega_m) + [\varepsilon_{k'} - \mu + \chi(k',i\omega_m)]^2 + \phi^2(k',i\omega_m)} \ , \tag{2a}$$

$$\chi(k,i\omega_m)=-\frac{1}{N}\sum_{k'}\frac{t_+(k,k')}{N(\mu)}\frac{\varepsilon_{k'}-\mu+\chi(k',i\omega_m)}{\omega_m^2 Z^2(k',i\omega_m)+[\varepsilon_{k'}-\mu+\chi(k',i\omega_m)]^2+\phi^2(k',i\omega_m)}\ , \tag{2b}$$

$$\phi(k,i\omega_m)=-\frac{1}{N\beta}\sum_{k',m'}V_{kk'}\frac{\phi(k',i\omega_{m'})}{\omega_{m'}^2 Z^2(k',i\omega_{m'})+[\varepsilon_{k'}-\mu+\chi(k',i\omega_{m'})]^2+\phi^2(k',i\omega_{m'})}$$
$$+\frac{1}{N}\sum_{k'}\frac{t_-(k,k')}{N(\mu)}\frac{\phi(k',i\omega_m)}{\omega_m^2 Z^2(k',i\omega_m)+[\varepsilon_{k'}-\mu+\chi(k',i\omega_m)]^2+\phi^2(k',i\omega_m)}\ . \tag{2c}$$

Here, Z and χ are contributions to the self-energy due to the impurities, and ϕ is the generalized pairing function. $N(\mu)$ is the density of states at the chemical potential and $t_\pm(k,k')\equiv t_N(k,k')\pm t_P(k,k')$, where

$$t_N(k,k')=n_N|\langle k|T_N|k'\rangle|^2N(\mu)\ , \tag{3a}$$

$$t_P(k,k')=n_PS(S+1)|\langle k|T_P|k'\rangle|^2N(\mu)\ . \tag{3b}$$

In Eqs. (3) the scattering potentials have been replaced by their T matrices. The normal (magnetic) impurity concentration is given by n_N (n_P), and S is the magnitude of the impurity spin. Eqs. (2a)–(2c) need to be supplemented with the occupancy condition for holes:

$$n=1-\frac{2}{N\beta}\sum_{k',m'}\frac{\varepsilon_{k'}-\mu+\chi(k',i\omega_{m'})}{\omega_{m'}^2 Z^2(k',i\omega_{m'})+[\varepsilon_{k'}-\mu+\chi(k',i\omega_{m'})]^2+\phi^2(k',i\omega_{m'})}\ . \tag{4}$$

Note that Hartree-Fock terms have been absorbed into the chemical potential and quasiparticle energy ε_k. In particular the mass enhancement as a function of doping is assumed to be included in the hopping matrix element t. This results in the replacement[17]

$$t\rightarrow t+n\Delta t\ , \tag{5}$$

so that the effective mass of holes is larger in more hole-like materials. In this paper, the on-site Coulomb repulsion U, as well as the off-diagonal Coulomb matrix element $\Delta t\equiv\alpha t$, is included in the Coulomb potential between two holes:

$$V_{kk'}\equiv U+2\alpha(\varepsilon_k+\varepsilon_{k'}) \tag{6}$$

Further-neighbor interactions can also be included in Eq. (6), but with little qualitative effect on the results. The attractive Hubbard model can be obtained by setting $\alpha\equiv0$ and U negative.

In Eqs. (3) the quantities $t_i(k,k')$ ($i=N,P$) are defined to include a conduction density of states, which is canceled upon insertion into Eqs. (2). This has been done to conform to standard notation, although, as will be seen below, such a practice can be very misleading. To proceed further we assume that the momentum dependence of the scattering matrix elements, $t_i(k,k')$ ($i=N,P$), can be ignored. One is then left with scattering probabilities, $t_i\equiv1/2\pi\tau_i$ ($i=N,P$), where τ_i is the lifetime due to impurity of type i. The momentum dependence of the unknown functions Z, χ, and ϕ is then considerably simplified:

$$Z(k,i\omega_m)=Z_m\ , \tag{7a}$$

$$\chi(k,i\omega_m)=\chi_m\ , \tag{7b}$$

$$\phi(k,i\omega_m)=\phi_k+\psi(m)\ , \tag{7c}$$

where

$$\phi_k\equiv\phi_0-\frac{\varepsilon_k}{D/2}\phi_1 \tag{7d}$$

and D is the bandwidth. To simplify the numerical computation, we adopt a constant-density-of-states model:

$$N(\varepsilon)=\frac{1}{D}\ ,\quad -\frac{D}{2}\le\varepsilon\le\frac{D}{2}\ , \tag{8}$$

which allows all momentum sums to be performed analytically. The resulting equations are tedious and are recorded in the Appendix. The T_c equation [Eq. (A7) in the Appendix] is

$$1+UT_0(T_c)-2KT_1(T_c)+K^2[T_1^2(T_c)-T_0(T_c)T_2(T_c)]=0\ , \tag{9}$$

where $K\equiv\alpha D$ and the T_l are defined in the Appendix. Some of the simple limiting cases are also derived there. In particular, in the absence of impurities, Eq. (9) becomes the T_c equation considered in previous work,[9] with $T_l\rightarrow I_l$ of Ref. 9(b). In the general case. Eq. (9) must be solved numerically.

As already mentioned, the presence of a modulated hopping term alters the electronic band structure [Eq. (5)]. We then expect that the strong-coupling regime ($T_c\gtrsim D$) may be appropriate in this model. In this case, assuming also that $Dt_{N,}Dt_P\ll T_c^2$, Eq. (9) can be simplified:

$$1+UZ(n)-\left[\frac{\alpha D}{2}\right]^2Y(n)Z(n)=0\ , \tag{10}$$

where

$$Y(n)=\frac{t_+D}{(2\pi T_c)^3}\frac{L_2(\mu)}{\pi}+\frac{n-1}{2\mu}\ , \tag{11a}$$

$$Z(n)=\frac{t_+D+t_-D}{(2\pi T_c)^3}\frac{L_2(\mu)}{\pi}+\frac{n-1}{2\mu}\ , \tag{11b}$$

and Eq. (4) becomes

$$\frac{n-1}{2\mu}=\frac{1}{2\pi T_c}\frac{L_1(\mu)}{\pi} -\frac{t_+D}{(2\pi T_c)^3}\left[\frac{3L_2(\mu)}{\pi}-4\left[\frac{\mu}{2\pi T_c}\right]^2\frac{L_3(\mu)}{\pi}\right] . \tag{11c}$$

In Eqs. (11a)–(11c), the L_i's are defined

$$L_i=\sum_{m=1}^{\infty}\frac{1}{[(m-\frac{1}{2})^2+\bar{\mu}^2]^i} , \quad i=1,2,3 \tag{12}$$

where $\bar{\mu}\equiv\mu/2\pi T_c$. The L_i's can be expressed in terms of hyperbolic tangents and secants. Then Eq. (11c), for example, becomes

$$n-1=\left[1-\frac{t_+D}{4T_c^2}n(2-n)\right]\tanh\pi\bar{\mu} , \tag{13}$$

which gives $\bar{\mu}$ as a function of hole concentration n. Analytical solutions to Eq. (11) will also be presented in the following sections.

III. NEGATIVE-U MODEL

In the negative-U model ($\alpha=0$), Eq. (9) is considerably simplified:

$$1=|U|T_0 . \tag{14}$$

The weak-coupling limit of this equation has been derived in the Appendix. In that limit, as is well known, normal impurities have no effect on T_c, whereas magnetic impurities are pair breaking, and T_c follows the Abrikosov-Gorkov[7] curve as a function of t_P. In the opposite limit (strong coupling), the situation is much different, and Eq. (10) becomes

$$1=|U|Z(n) , \tag{15}$$

where $Z(n)$ is given by Eq. (11b), and, to lowest order in $t_{\pm}D$ we find

$$L_2(n)=\frac{\pi^4}{4}\frac{f^2(n)}{(1-n)^2}[f(n)-n(2-n)] , \tag{16}$$

where $f(n)=2(1-n)/\ln[(2-n)/n]$. Note that $\lim_{n\to 1}f(n)=1$ and $\lim_{n\to 1}L_2(n)=\pi^4/6$. From Eq. (16) we obtain

$$Z(n)=\frac{n-1}{2\mu}+\frac{t_+D+t_-D}{32T_c^3}\frac{f^2(n)}{(1-n)^2}[f(n)-n(2-n)] . \tag{17}$$

Let us denote the solution in the absence of impurities with a subscript "0." Then $\mu=\mu_0+\delta\mu$ and $T_c=T_{c0}+\delta T_c$, and we obtain from Eqs. (15), (17), and (13)

$$\frac{\delta T_c}{T_{c0}}=-g_i(n)\frac{D}{|U|}\frac{t_i}{T_{c0}} , \tag{18}$$

where $g_N(n)=[1-f(n)]/(1-n)^2$, and $g_P(n)=1$. Since $f(n)\le 1$ for all n, both normal and magnetic impurities are pair breaking in the strong-coupling limit. In particular, $\lim_{n\to 1}g_N(n)=\frac{1}{3}$, so that at half-filling, T_c is reduced by normal impurities $\frac{1}{3}$ as effectively as by magnetic impurities. In the dilute limit ($n\to 0$) both kinds of impurities become equally effective. In Fig. 1 we show $g_N(n)$ vs n, which illustrates the pair-breaking effect of normal impurities as a function of occupation in the strong-coupling limit. The effect from both types of impurities becomes comparable only in the extreme dilute limit. In Fig. 2 we show numerical results of T_c/T_{c0} vs t_i/T_{c0} for both normal and magnetic impurities, for various bandwidths. We have used $D=5.0$, 0.1, and 0.02 eV, and $|U|$ has been chosen in each case to give $T_{c0}=100$ K. In Fig. 2(a) the occupation has been fixed at half-filling, whereas in Fig. 2(b), $n=0.1$. It is apparent that the strong-coupling limit [Eq. (18)] is achieved only when the bandwidth becomes comparable to T_{c0}. Otherwise, magnetic impurities are far more detrimental to T_c than Eq. (18) might indicate. In particular, in Fig. 2(a), the Abrikosov-Gorkov curve is reproduced for $D=5.0$ eV, with a critical scattering strength, $t_P^*\approx 0.14T_{c0}$.

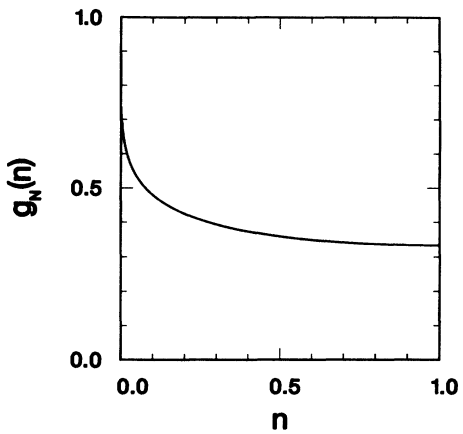

FIG. 1. The universal function $g_N(n)$ vs occupation n. $g_N(n)$ describes the reduction in T_c caused by normal impurities relative to magnetic ones within the negative-U model, in the strong-coupling limit. For most of the occupation regime, magnetic impurities are 2–3 times more effective pair breakers. In the extreme dilute limit $g_N(n)$ approaches unity logarithmically.

In Fig. 2 we have compared normal and magnetic pair-breaking effects for a given bandwidth. Comparing the results for various bandwidths would lead one to conclude that a narrower band-width gives rise to less pair breaking. In order to investigate the dependence on bandwidth itself, however, it is more appropriate to plot T_c/T_{c0} vs Dt_i/T_{c0}^2. In this way the explicit dependence on the density of states contained in Eqs. (3a) and (3b) is removed, and Dt_i/T_{c0}^2 is an unbiased measure of the impurity concentration and/or scattering strength. In Fig. 3 we show results for the dependence of T_c on both magnetic and normal impurities, for the same three bandwidths plotted with abscissa Dt_i/T_{c0}^2. It is then clear that a *narrower* bandwidth gives rise to *increased* pair breaking. This is expected since considerably more smearing and therefore lowering of the density of states occurs for a narrower bandwidth.

To display the full dependence of pair breaking on bandwidth, we plot in Fig. 4, the initial slope

$$m_i \equiv |\partial(T_c/T_{c0})/\partial(Dt_i/T_{c0}^2)|$$

for $i=N,P$ vs T_{c0}/D, in the negative-U model at half filling. Since $T_c/T_{c0}=f(T_{c0}/D, Dt_i/T_{c0}^2)$, these are universal curves. The solid line represents the pair breaking due to magnetic impurities, the dashed line that due to normal impurities. In the weak-coupling limit, normal impurities have no first-order effect. In Fig. 4 this is clear from the fact that the dashed line approaches the origin with zero slope. On the other hand, the solid curve approaches the origin with a nonzero slope. For low concentration of impurities, expression (A15) gives

$$\frac{T_c}{T_{c0}} = 1 - \frac{\pi^2}{2}\frac{T_{c0}}{D}\left[\frac{Dt_P}{T_{c0}^2}\right] . \tag{19}$$

The initial slope of the solid line in Fig. 4 is approximately $\pi^2/2$, in agreement with this result. In the strong-coupling limit the two curves approach $\frac{1}{4}$ and $\frac{1}{12}$, respectively, as Eq. (18) and Fig. 1 imply.

To summarize this section we note that within the negative-U model, both magnetic and nonmagnetic impurities are pair breaking in the intermediate- and strong-coupling regime. This remains true for all occupations. Unfortunately, the BCS solution to this model is not expected to be physical in this regime. Instead, the

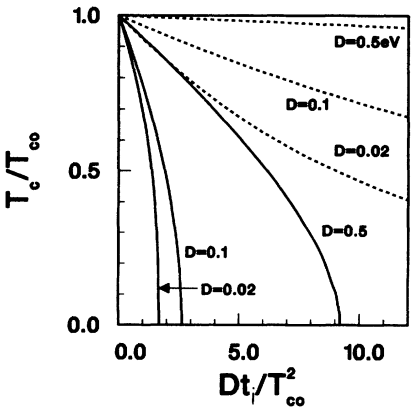

FIG. 3. T_c/T_{c0} vs Dt_i/T_{c0}^2 $(i=N,P)$ for the negative-U model at half filling, for the bandwidths indicated using $n=1$ and $T_{c0}=100$ K. The widest bandwidth corresponds to weak coupling while the narrowest corresponds to strong coupling. We have used Dt_i/T_{c0}^2 for the abscissa in order to remove the dependence on the conduction band density of states [see Eq. (3)]. As before solid (dashed) lines correspond to magnetic (normal) impurities. A smaller bandwidth enhances pair breaking. Note that the strong-coupling limit [Eq. (18)] only applies for $Dt_i/T_{c0}^2 \lesssim 1$, where the results are linear.

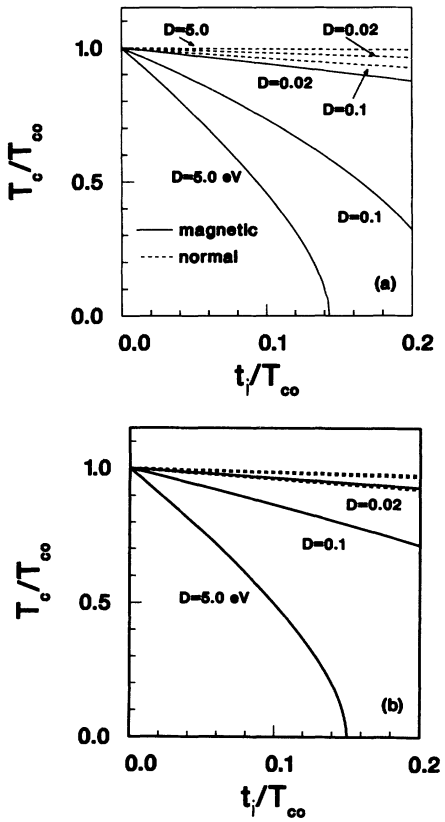

FIG. 2. Critical temperature ratio T_c/T_{c0} vs t_i/T_{c0} $(i=N,P)$ in the negative-U model for occupations (a) $n=1.0$ and (b) $n=0.1$, for various bandwidths. Solid (dashed) lines are for $i=P$ (N). In weak coupling $(D \gg T_{c0})$ only magnetic impurities are pair breaking. In strong coupling, the curves approach the behavior indicated by Eq. (18). In (a) the bandwidths for each curve are given; in (b) the solid curves are labeled with their bandwidths. The lowest dashed curve is for bandwidth $D=0.1$ eV and the two uppermost curves are for $D=0.02$ and 5.0 eV. In each case U is determined from the condition $T_{c0}=100$ K.

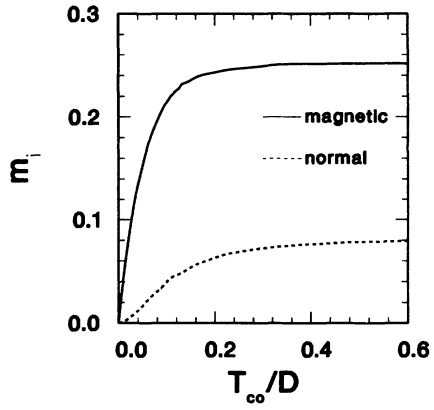

FIG. 4. The absolute value of the slope, $m_i \equiv |\partial(T_c/T_{c0})/\partial(Dt_i/T_{c0})^2|$ $(i=N,P)$ vs T_c/D. Weak coupling is to the left of the diagram, strong coupling is to the right. The solid (dashed) line is for magnetic (normal) impurities. Even though both curves approach the origin, magnetic impurities are pair breaking in weak coupling due to the finite slope of the solid line, whereas normal impurities are not. In strong coupling m_P (m_N) approaches $\frac{1}{4}$ $(\frac{1}{12})$. Note that these curves represent the initial slopes on the results displayed in Fig. 3, so these results apply only in the linearized regime. This result applies to half filling $(n=1)$, and is universal.

transition is expected to occur via Bose condensation. In the weak-coupling regime the BCS solution to the negative-U model is expected to be accurate. Here, magnetic impurities are pair breaking and normal impurities have only a small pair-breaking effect. In the following section we discuss a model in which normal impurities have a strong pair-breaking effect in a regime that is believed to be physically relevant, and accurately described by BCS theory.

IV. HOLE MECHANISM

When K is nonzero, Eqs. (9) and (4) must be iterated numerically to determine T_c as a function of both impurity concentration and hole occupation. Before presenting numerical results we first review some previous work[9] and derive the strong-coupling limit analytically in analogy to the negative-U model. $T_c(n)$, as determined in this theory, is nonzero only for a narrow region of hole occupation: $0<n\lesssim 0.2$. The reason for this is that the terms in the effective hole potential proportional to α [see Eq. (6)] are most attractive when the momenta are such that the eigenvalues lie near the bottom of the hole band. The linear increase in potential as a function of energy yields a gap function that is monotonically decreasing (increasing) as a function of energy in the hole (electron) picture [see Eq. (7d)]. It is important to emphasize that the gap remains isotropic, that is, it is constant over constant-energy surfaces. Therefore, within this model, impurities *do not* effect T_c through the standard mechanism of washing out anisotropy.[18] The reason we expect impurities to have a direct influence on T_c is that Anderson's argument[6] does not carry through when states well away from the Fermi surface also contribute to the pairing interaction in a nontrivial way. As the electron eigenstates are readjusted by impurities the pairing interaction remains rigid across the entire bandwidth; in contrast, in the usual scenario, the constant pairing potential "tracks" the Fermi level, leading to no change in T_c.

It is useful to obtain analytically the T_c correction due to impurities to lowest order in t_i/T_{c0}, in the strong-coupling regime. As before, the occupancy condition is given by Eq. (13). The function $Z(n)$ is given by Eq. (17) and $Y(n)$ is given by a similar expression [see Eqs. (11)]. Carrying through the same expansion as before, we obtain

$$\frac{\delta T_c}{T_{c0}}=-\frac{D}{4T_{c0}}f(n)\left[\frac{t_N+t_P}{T_{c0}}\left[1-\frac{1}{2}\frac{f(n)-n(2-n)}{(1-n)^2}\right]-\frac{t_N-t_P}{T_{c0}}\frac{f(n)-n(2-n)}{2(1-n)^2}\frac{1}{2+(U/4T_{c0})f(n)}\right]. \tag{20}$$

Physically, we expect $U\gg T_{c0}$ always, so that the second term in Eq. (20) is negligible. This implies that for all fillings *normal impurities are as equally pair breaking as magnetic impurities.* For $U\gg T_{c0}$, we write

$$\frac{\delta T_c}{T_{c0}}=-\frac{1}{6}\left[\frac{D(t_N+t_P)}{T_{c0}^2}\right]g(n)\ , \tag{21}$$

where

$$g(n)=\frac{3}{2}f(n)\left[1-\frac{f(n)-n(2-n)}{2(1-n)^2}\right]. \tag{22}$$

A plot of $g(n)$ vs n is shown in Fig. 5. In this model

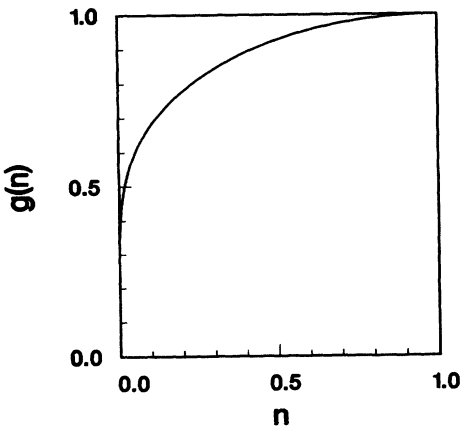

FIG. 5. The universal function $g(n)$ vs n for the hole mechanism, in the strong-coupling limit.

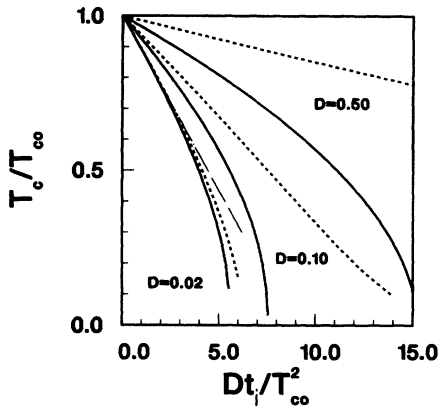

FIG. 6 T_c/T_{c0} vs Dt_i/T_{c0}^2 for three different bandwidths, $D=0.5$, 0.1, and 0.02 eV. Here, $U=5$ eV, $n=0.1$, and Δt has been chosen to yield $T_{c0}=100$ K. Solid (dashed) lines denote magnetic (normal) impurity scattering. As the bandwidth decreases, T_c suffers a greater reduction for given impurity concentration and the effects of magnetic and normal impurity scattering become the same. The dashed-dotted line indicates the strong-coupling limit (applicable for small Dt_i/T_{c0}^2). It is clear that this limit has been achieved for $D=0.02$ eV.

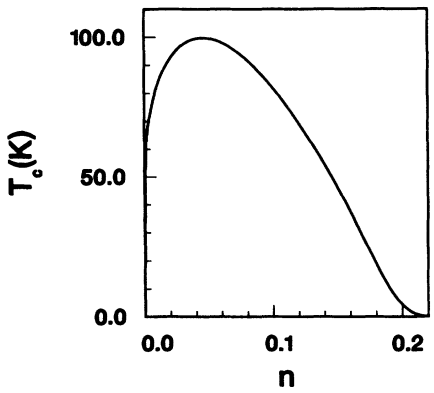

FIG. 7. Critical temperature T_c vs hole occupation n. Here $U=5$ eV, $t_h=0.001$ eV, and $\Delta t=0.135$. The parameters were chosen to give a maximum $T_c=100$ K. The effective bandwidth changes as a function of occupation, as described in the text and in Table I.

the physically relevant occupation regime is $0<n\lesssim 0.2$ (see Ref. 9 and below). Note that, contrary to the result for the negative-U model, in the strong-coupling limit, normal impurities are more effective pairbreakers for *larger* n. It is worth emphasizing that in this model the strong-coupling limit is physically relevant, due to the hopping renormalization that occurs.[19]

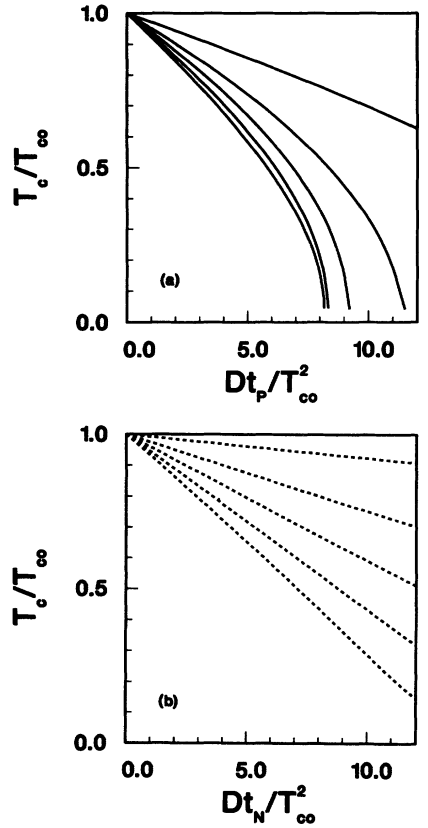

FIG. 8. T_c/T_{c0} vs Dt_P/T_{c0}^2 in (a) and Dt_N/T_{c0}^2 in (b), for the last five occupations listed in Table I. In both cases the hole occupation decreases as the curves progress from top to bottom. At the lowest occupations shown T_c/T_{c0} becomes comparable for both normal and magnetic impurities.

TABLE I. Effective bandwidths (in eV) and $T_{c0}(n)$ for various hole occupations (see Fig. 7). $U=5.0$ eV, $\Delta t=0.135$ eV, and $t_h=0.001$ eV.

n	$D(n)$	T_{c0} (K)	T_{c0}/D
0.03	0.005	97.3	0.207
0.06	0.009	98.1	0.116
0.09	0.013	87.3	0.072
0.12	0.017	69.5	0.044
0.15	0.021	46.6	0.024
0.18	0.025	19.2	0.008

In order to investigate the effects of the different types of impurities in the weak- and intermediate-coupling regimes, we have solved the T_c equations numerically, using different bandwidths, as a function of Dt_i/T_{c0}^2. Figure 6 illustrates the renormalized reduction of T_c for $D=0.5$, 0.1, and 0.02 eV. Solid (dashed) lines denote magnetic (nonmagnetic) impurities. In each case we have used $n=0.1$ and $U=5.0$ eV, and Δt has been adjusted to give $T_{c0}=100$ K. Also included is the strong-coupling result from Eq. (21), indicated by the dashed-dotted line. Clearly the strong-coupling result is already achieved for $D=0.02$ eV. For weaker-coupling strengths T_c is more effectively reduced by magnetic impurities. We have also obtained solutions for $U=10$ eV again adjusting Δt to give $T_{c0}=100$ K. The results are nearly indistinguishable from the cases shown.

It is also important to examine the influence of impurities on T_c as a function of occupation, for a given set of parameters. In Fig. 7 we show T_c vs n for $U=5.0$ eV, $\Delta t=0.135$ eV, and $t_h=0.001$ eV, where t_h is the hopping at the bottom (top) of the hole (electron) band. The parameters have been chosen to give a maximum T_c of 100 K at $n=0.045$, and to approach the strong-coupling limit as $n\to 0$. The T_c vs n curve has the familiar maximum at very low hole filling, as discussed previously.[9] Table I lists the parameters for representative hole concentrations. In Fig. 8 we show plots of T_c/T_{c0} vs Dt_i/T_{c0}^2 for

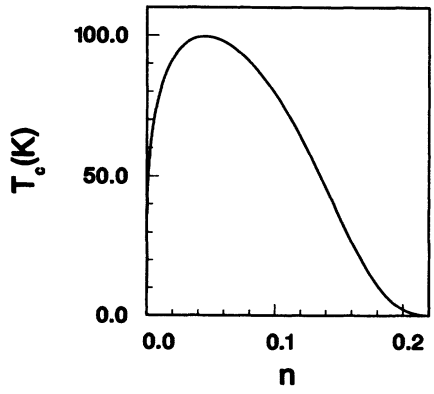

FIG. 9. T_c vs n for $U=5$ eV, $t_h=0.03$ eV, and $\Delta t=0.1875$. The result is similar to that in Fig. 7.

TABLE II. Effective bandwidths (in eV) and $T_{c0}(n)$ for various hole occupations (see Fig. 9). $U=5.0$ eV, $\Delta t=0.1875$ eV, and $t_h=0.03$ eV.

n	$D(n)$	T_{c0} (K)	T_{c0}/D
0.03	0.285	97.0	0.029
0.06	0.330	97.9	0.026
0.09	0.375	85.6	0.020
0.12	0.420	64.3	0.013
0.15	0.465	36.3	0.007
0.18	0.510	11.0	0.002

the occupations listed in Table I. In particular, Figs. 8(a) and 8(b) show the separate effects of magnetic and nonmagnetic impurities, respectively. In both cases the largest occupation is given by the uppermost curve. As occupation decreases, T_c/T_{c0} decreases as a function of hole concentration for given impurity concentration. For clarity we have omitted the result for $n=0.03$. For the lowest occupations, both kinds of impurities initially have a similar effect on T_c. For extremely low occupations (not shown) the initial slope is given by Eq. (21), and then there is a very slight reversal of the above trend with hole concentration as the curves follow the behavior indicated

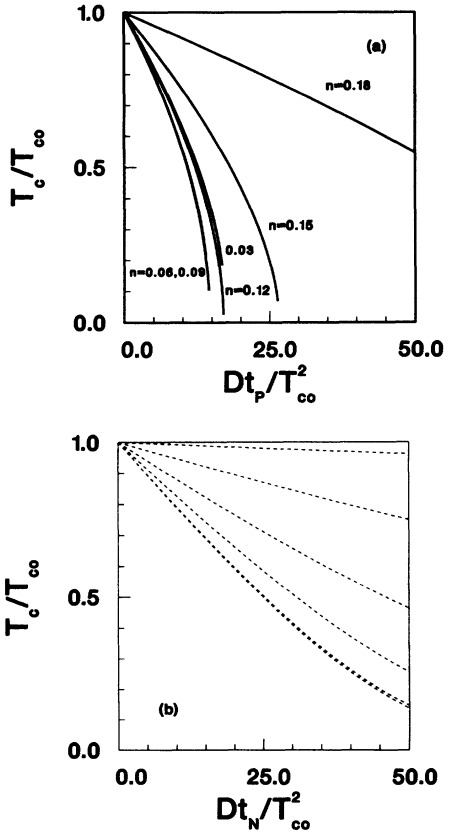

FIG. 10. T_c/T_{c0} vs Dt_P/T_{c0}^2 in (a) and Dt_N/T_{c0}^2 in (b), for the hole occupations listed in Table II. At the lowest occupation there is a nonmonotonic dependence of T_c/T_{c0} on hole occupation in the case of magnetic impurity scattering.

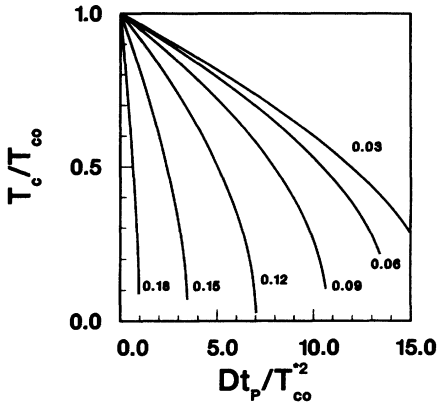

FIG. 11. T_c/T_{c0} vs Dt_P/T_{c0}^{*2} where $T_{c0}^*\equiv 100$ K, for the parameters listed in Table II and the figure caption in Fig. 9. Magnetic impurities reduce T_c more effectively for higher hole occupations than for low occupations.

by Fig. 5 (less pair breaking for lower hole occupation). As the occupation is increased there is a crossover to the weak-coupling limit (see Ref. 20 for a full discussion of this crossover) and magnetic impurities have a more detrimental effect than nonmagnetic ones on T_c. Nonetheless, normal impurities continue to be pair breaking.

In Figs. 9 and 10 we provide similar results for a different set of parameters: $U=5.0$ eV, $\Delta t=0.1875$ eV, and $t_h=0.03$ eV. Again, these were chosen to give a maximum T_c of 100 K at $n=0.045$, but now the theory is in the weak-coupling regime for the entire hole concentration range. Relevant parameters for various hole occupations are listed in Table II. In Fig. 9, T_c is shown versus hole occupation. The result is very similar to that of Fig. 7. In Fig. 10(a) [Fig. 10(b)] we show the effects due to magnetic (normal) impurities for a range of hole concentrations. Again, the pair breaking is generally greater for decreasing hole concentration, since as hole concentration decreases the bandwidth decreases and the regime is stronger coupling. For the lowest occupation shown ($n=0.03$), however, the trend has reversed itself, and magnetic impurities are less pair breaking than for somewhat higher concentrations. This is the same behavior alluded to in Fig. 8.

Fujishita and Sato[21] have studied the compound $La_{2-y}Sr_yCu_{1-x}Ni_xO_4$ as a function of y and x. Assuming Ni acts as a magnetic pair-breaking impurity, it is interesting to compare our results with experiment. Fujishita and Sato[21] examined the effect of Ni substitution for compounds with three nominal hole concentrations, $y=0.10$, 0.15, and 0.22. They found that, as hole concentration increases, the same concentration of Ni is less pair breaking (see Fig. 5 of Ref. 21). To compare with our results it is necessary to plot T_c/T_{c0} vs Dt_p/T_{c0}^{*2} where T_{c0}^* is some *fixed* temperature. In this way Dt_p/T_{c0}^{*2} reflects only the impurity concentration and/or scattering length. In Fig. 11 we show T_c/T_{c0} vs Dt_p/T_{c0}^{*2} for the parameters of Fig. 10 (see Table II). It is clear that as hole concentration increases, the pair breaking also increases, in disagreement with the experimental re-

sult. Similar behavior is found for normal impurities, and for the strong-coupling case given in Table I.

V. SUMMARY

We have investigated the effects of both normal and magnetic impurity scattering on the superconducting transition temperature T_c within the theoretical framework of the hole mechanism of superconductivity.[9] Since the standard BCS treatment assumes an infinite bandwidth, we have also investigated the effects of finite bandwidth by studying the negative-U model. We have found that in the strong-coupling limit ($D \ll T_c$), both magnetic and normal impurities are pair breaking. Over most of the possible occupation regime, magnetic impurities are more effective than normal ones by a factor of 2–3. However, the regime of the negative-U model over which this occurs is probably unphysical and inaccurately described by BCS theory. In the more physical weak-coupling regime, normal impurities are not very effective pair breakers.

The value of T_c, as determined within the hole mechanism, is expected to be more sensitive to impurities due to the intrinsic energy dependence of the gap function. Our calculations have verified that this is so. For weak coupling, there is again a significant discrepancy in pair-breaking effectiveness between magnetic and normal impurities. In intermediate and strong coupling, however, both impurities cause an equivalent reduction in T_c, provided the Hubbard U is large compared to T_c. We emphasize, once again, that the strong-coupling regime arises in a very natural way in this theory, since the effective mass is expected to be very large in the low-hole-doping regime. Furthermore, the pair dissociation will remain of the BCS type,[19] so that this theory remains accurate in strong coupling. In light of these results one is led to interpret the observed reduction in T_c as a function of both normal and magnetic impurity alloying as evidence in favor of the hole mechanism of superconductivity. A significant discrepancy with experiment remains, however. Fujishita and Sato[21] find precisely the opposite behavior as a function of hole concentration (in $La_{2-y}Sr_yCu_{1-x}Ni_xO_4$) compared to what we predict in Fig. 11. We find that the pair breaking due to magnetic impurities increases as the hole concentration is increased, whereas they find the opposite. Perhaps these impurities play a more important role than just elastic-scattering centers. Experiments similar to that of Fujishita and Sato[21] on other high-T_c compounds would be beneficial.

ACKNOWLEDGMENT

The author thanks Jorge Hirsch for first suggesting that normal impurities should be pair breaking within this mechanism, and for helpful discussions thereafter.

APPENDIX

For a constant density of states and a momentum-independent scattering matrix, the solution of the linearized Eqs. 2(a)–(2c) requires the integrals

$$J_l(m) \equiv \frac{1}{D}\int_{-D/2}^{D/2} d\varepsilon \frac{[-\varepsilon/(D/2)]^l}{\tilde{\omega}_m^2+(\varepsilon-\mu+\chi_m)^2}, \quad l=0,1,2 \tag{A1}$$

where $\tilde{\omega}_m \equiv \omega_m Z_m$. We find

$$J_0(m)=\frac{\pi}{D}\frac{A(m)}{|\tilde{\omega}_m|}, \tag{A2a}$$

$$J_1(m)=-\left[\frac{\mu-\chi_m}{D/2}\right]J_0(m)-\frac{B(m)}{D^2}, \tag{A2b}$$

and

$$J_2(m)=\frac{1}{(D/2)^2}\left[1-[\tilde{\omega}_m^2-(\mu-\chi_m)^2]\frac{\pi}{D}\frac{A(m)}{|\tilde{\omega}_m|}+(\mu-\chi_m)\frac{B(m)}{D}\right], \tag{A2c}$$

where

$$A(m)=\frac{1}{\pi}\left[\tan^{-1}\left[\frac{D/2-\mu+\chi_m}{|\tilde{\omega}_m|}\right]+\tan^{-1}\left[\frac{D/2+\mu-\chi_m}{|\tilde{\omega}_m|}\right]\right] \tag{A3a}$$

and

$$B(m)=\ln\left[\frac{\tilde{\omega}_m^2+(D/2-\mu+\chi_m)^2}{\tilde{\omega}_m^2+(D/2+\mu-\chi_m)^2}\right]. \tag{A3b}$$

Equations (2a), (2b), and (4) then become, respectively

$$\tilde{\omega}_m=\omega_m+\pi t_+ A(m)\,\mathrm{sgn}\omega_m, \tag{A4a}$$

$$\chi_m=-\frac{t_+}{2}B(m), \tag{A4b}$$

and

$$n=1-\frac{2}{\beta}\sum_{m=1}^{\infty}\frac{B(m)}{D}. \tag{A4c}$$

Equation (2c) is a little more tedious to handle. Using the decomposition defined in Eqs. (7c) and (7d), we have

$$\psi(m)=t_-\int_{-D/2}^{D/2} d\varepsilon \frac{\psi(m)+\phi_0-[\varepsilon'/(D/2)]\phi_1}{\tilde{\omega}_m^2+(\varepsilon-\mu+\chi_m)^2}, \tag{A5a}$$

$$\phi_0=-\frac{2}{\beta}\sum_{m=1}^{\infty}\int_{-D/2}^{D/2} d\varepsilon'\left[\frac{U}{D}+\alpha\frac{\varepsilon'}{D/2}\right]\times\frac{\psi(m)+\phi_0-[\varepsilon'/(D/2)]\phi_1}{\tilde{\omega}_m^2+(\varepsilon'-\mu+\chi_m)^2}, \tag{A5b}$$

and

$$\phi_1=\frac{2\alpha}{\beta}\sum_{m=1}^{\infty}\int_{-D/2}^{D/2} d\varepsilon'\frac{\psi(m)+\phi_0-[\varepsilon'/(D/2)]\phi_1}{\tilde{\omega}_m^2+(\varepsilon'-\mu+\chi_m)^2}. \tag{A5c}$$

From Eq. (A5a), the explicit solution for $\psi(m)$ is

$$\psi(m)=\frac{Dt_-}{1-Dt_-J_0(m)}[\phi_0 J_0(m)+\phi_1 J_1(m)] , \quad \text{(A6)}$$

which can then be substituted into Eqs. (A5b) and (A5c). All the energy integrations can be performed analytically, in terms of $J_l(m)$, $l=0,1,2$. The resulting T_c equation is

$$1-2KT_1(T_c)+UT_0(T_c)+K^2[T_1^2(T_c)-T_0(T_c)T_2(T_c)] =0 , \quad \text{(A7)}$$

where

$$T_0=\frac{2}{\beta}\sum_{m=1}^{\infty}\frac{J_0(m)}{1-t_-DJ_0(m)} , \quad \text{(A8a)}$$

$$T_1=\frac{2}{\beta}\sum_{m=1}^{\infty}\frac{J_1(m)}{1-t_-DJ_0(m)} , \quad \text{(A8b)}$$

and

$$T_2=\frac{2}{\beta}\sum_{m=1}^{\infty}\left[J_2(m)+\frac{t_-D}{1-t_-DJ_0(m)}J_1^2(m)\right] . \quad \text{(A8c)}$$

In practice, the sums occurring in Eqs. (8a)–(8c) are done numerically up to some large cutoff, while the remaining portion to infinity is performed analytically using asymptotic expansions for the functions involved. Equation (A7) is iterated to convergence as a function of temperature in order to find a solution, while at each temperature Eqs. (A4a)–(A4c) are iterated to determine $\tilde{\omega}_m$, χ_m, and μ, for a given filling.

It is useful to recover some well-known limits from these equations. With no impurities, $\chi_m=0$, and $\tilde{\omega}_m=\omega_m$, and using Eqs. (A9a) and (A1), one can perform the Matsubara sum first, leaving behind energy integrations so that one finds

$$T_l \to I_l , \quad \text{(A9)}$$

where I_l are the sums defined by Eq. (11) in Ref. 9(b), with the same T_c equation.

The standard Abrikosov-Gorkov result is also obtained, taking $\alpha=0$, $U=-|U|$, $\mu=0$ (half filling), and $D\gg T_c,t_\pm$. Then $A(m)\to 1$, $B(m)\to 0$, $\chi_m=0$, and $\tilde{\omega}_m\to\omega_m+\pi t_+\,\mathrm{sgn}\omega_m$. The limit $D\gg T_c,t_\pm$, must be taken with care. We have from Eq. (A7)

$$\frac{1}{|U|}=T_0=2T_c\sum_{m=1}^{\infty}\frac{1}{J_0^{-1}(m)-t_-D} . \quad \text{(A10)}$$

In order to use $J_0(m)\approx\pi/(D\tilde{\omega}_m)$, we must also sum to infinity using a well-defined limiting procedure:

$$\frac{1}{|u|}=2\pi T_c\lim_{D\to\infty}\sum_{m=1}^{N_D}\frac{1}{\omega_m+2\pi t_p} , \quad \text{(A11)}$$

where $|u|=|U|/D$, and $N_D=D/2\pi T_c+\frac{1}{2}$. Normal impurities have dropped out of the T_c equation, as is well known. Now we follow the standard procedure, using

$$\frac{1}{|u|}=2\pi T_{c0}\lim_{D\to\infty}\sum_{m=1}^{N_{D0}}\frac{1}{\omega_{m0}} , \quad \text{(A12)}$$

where the added subscript "0" indicates an absence of impurities. We find

$$\lim_{D\to\infty}\psi\left[\frac{D}{2\pi T_{c0}}+\frac{1}{2}\right]-\psi\left[\frac{1}{2}\right] =\lim_{D\to\infty}\psi\left[\frac{D}{2\pi T_c}+\frac{1}{2}+\frac{t_p}{T_c}\right]-\psi\left[\frac{1}{2}+\frac{t_p}{T_c}\right] , \quad \text{(A13)}$$

where $\psi(z)$ is the digamma function. Since $\lim_{z\to\infty}\psi(z+\frac{1}{2})\sim\ln z$, we recover the familiar Abrikosov-Gorkov[7] expression

$$\ln\left[\frac{T_{c0}}{T_c}\right]=\psi\left[\rho_c+\frac{1}{2}\right]-\psi\left[\frac{1}{2}\right] , \quad \text{(A14)}$$

where $\rho_c=t_P/T_c=1/2\pi\tau_P T_c$. For low concentration of impurities, $1/\tau_P\ll T_c$, we find

$$\frac{T_c}{T_{c0}}=1-\frac{\pi}{4}\frac{1}{\tau_P T_{c0}} , \quad \text{(A15)}$$

which is equivalent to Eq. (19) in the text.

[1] J. B. Torrance, Y. Tokura, A. I. Nazzal, A. Bezinge, T. C. Huang, and S. S. P. Parkin, Phys. Rev. Lett. **61**, 1127 (1988).

[2] N. Tanahashi, Y. Iye, T. Tamegai, C. Murayama, N. Mori, S. Yomo, N. Okazaki, and K. Kitazawa, J. Appl. Phys. **28**, L762 (1989).

[3] H. Takagi, T. Ido, S. Ishibashi, M. Uota, S. Uchida, and Y. Tokura, Phys. Rev. B **40**, 2254 (1989).

[4] G. Xiao, F. M. Streitz, A. Gavrin, Y. W. Du, and C. L. Chien, Phys. Rev. B **35**, 8782 (1987). More recently, see G. Xiao *et al.*, *ibid.* **42**, 8752 (1990); Y. Maeno, T. Tomita, M. Kyogoku, S. Awaji, Y. Aoki, K. Moshino, A. Minami, and T. Fujita, Nature **328**, 512 (1987); J. M. Tarascon, P. Barboux, P. F. Miceli, L. M. Greene, G. W. Hull, M.Eibschutz, and S. A. Sunshine, Phys. Rev. B **37**, 7458 (1988). Many other investigations have been reported, but these are too numerous to list here.

[5] Cu nominally has a spin-$\frac{1}{2}$ magnetic moment, so that it is not clear exactly what the magnetic nature of a spin-1 Ni impurity is vs a spin-zero Zn substitution. The author thanks E. A. Early for bringing this fact to his attention. Nevertheless in the remainder of the paper we will proceed calling the Ni-type substitution "magnetic" and the Zn-type one "nonmagnetic."

[6] P. W. Anderson, J. Phys. Chem. Solids **11**, 26 (1959).

[7] A. A. Abrikosov and L. P.Gor'kov, Zh. Eksp. Teor. Fiz. **35**, 1558 (1958) [Sov. Phys. JETP **8**, 1090 (1959)].

[8] J. E. Hirsch, Phys. Lett. A **134**, 451 (1989).

[9] (a) J. E. Hirsch and F. Marsiglio, Phys. Rev. B **41**, 2049 (1990); (b) **39**, 11 515 (1989); (c) F. Marsiglio and J. E. Hirsch, *ibid.* **41**, 6435 (1990).

[10]A. Zawadowski, Phys. Scr. **T27**, 66 (1989).
[11]V. A. Ivanov and R. O. Zaitsev, Int. J. Mod. Phys. B **1**, 689 (1988).
[12]R. Micnas, J. Ranninger, and S. Robaszkiewicz, Phys. Rev. B **39**, 11 653 (1989).
[13]G. Baskaran, Z. Zou, and P. W. Anderson, Solid State Commun. **69**, 973 (1987).
[14]A. E. Ruckenstein, P. J. Hirschfeld, and J. Appel, Phys. Rev. B **36**, 857 (1987).
[15]L. Coffey and D. L.Cox, Phys. Rev. B **37**, 3389 (1988). I wish to thank Professor Dan Cox for bringing this work to my attention.
[16]P. B. Allen and B. Mitrović, in *Solid State Physics,* edited by H. Ehrenreich, F. Seitz, and D. Turnbull (Academic, New York, 1982), Vol. 37, p. 1.
[17]J. E. Hirsch, Physica C **158**, 326 (1989).
[18]D. Markowitz and L. P. Kadanoff, Phys. Rev. **131**, 563 (1963).
[19]J. E. Hirsch, Physica C **161**, 185 (1989).
[20]F. Marsiglio and J.E. Hirsch, Physica C **165**, 71 (1990).
[21]H. Fujishita and M. Sato, Solid State Commun. **72**, 529 (1989).